JOURNAL OF MATERIALS SCIENCE 35 (2000) 3903–3912

High temperature behaviour of a Ti-6Al-4V/TiC_p composite processed by BE-CIP-HIP method

C. BADINI, G. UBERTALLI, D. PUPPO, P. FINO
Politecnico di Torino, Dip. di Scienza dei Materiali e Ingegneria Chimica C.so Duca degli Abruzzi 24, 10129 Torino, Italy
E-mail: badini@athena.polito.it

The high temperature behaviour of a Ti-6Al-4V/TiC_p composite (10% Vol. of TiC) was investigated. A composite produced by Dynamet Technology according to the blended-elemental-cold-hot isostatic pressing (BE-CHIP) method was used. The stress-strain properties of the material were tested at 25, 200, 400, 500, 600 and 800°C. Composite specimens were aged in air at 500 and 700°C or under vacuum at 500, 700 and 1050°C, for periods ranging between 100 and 500 hours. The thermal stability of the matrix/ceramic interfaces was studied by using scanning electron microscope, electron probe microanalysis and x-ray diffraction. Carbon diffusion from the ceramic particles towards the composite matrix occurred (very likely already during the composite fabrication) because the metal matrix of all the composite samples (either in the as received or thermally treated conditions) showed a high content of carbon (more than 1% at.). However, the thermal treatments carried out at both 500 and 700°C under vacuum did not result in a ceramic-metal reaction. In spite of this, the formation of an ordered phase of formula Ti_2C can be inferred. Long period aging under vacuum at 700°C (500 h) did not lower the composite tensile strength. On the other hand, above 500°C in air the titanium matrix rapidly underwent oxidation, which gave rise to the formation of a thick surface reaction layer; this confirms that the composite material cannot be used above this temperature. Furthermore, the thermal treatment performed at 1050°C (under vacuum) resulted in a strong composite microstructure modification: the formation of new mixed carbides of Al and Ti was observed.

1. Introduction

In the last years new low-cost methods for the production of titanium-alloy/ceramic-particle composites have been developed. These fabrication routes were derived from the blended elemental (BE) method, used for processing unreinforced titanium components by powder metallurgy [1]. Cheap particle-reinforced composites have been produced according to the following steps: blending of the elemental powders, compaction by cold isostatic pressing and sintering [2] or compaction by hot isostatic pressing [3–5]. Several ceramic particles were proposed as titanium reinforcement: SiC, B_4C, TiAl, TiB_2, TiN, TiC and TiB. According to some investigations (chiefly performed at Toyota industries) the best results can be achieved by using TiB. Moreover, according to Dynamet researches, composites with superior properties can also be obtained through the BE-CHIP process by using TiC or TiB_2 particles as reinforcement [6–10]. These composites (CermeTi®) show higher Young modulus and yield strength than the corresponding unreinforced alloys (in particular at high temperatures), useful level of fracture toughness (K_{Ic} ranging with the ceramic content between 25 and 40 MPa $m^{1/2}$), high hardness and wear resistance, excellent creep properties.

Due to their mechanical properties, the low-cost and low-density CermeTi composites seem suitable for applications in aerospace and automotive fields. As mentioned above, one of the more interesting characteristic of these composites is that of retaining good mechanical properties at rather high temperatures. Moreover, common titanium alloys can generally be used at temperature of about 500°C; higher temperatures can be sustained by β titanium alloys containing tailored alloying elements. For this reasons, the Ti/ceramic-particles composites should present important advantages over the aluminium-based MMCs, provided that detrimental reactions do not occur between matrix and ceramic at high temperatures.

This paper deals with the thermal stability of a Ti-6Al-4V/TiC_p composite and its high temperature mechanical behaviour.

2. Experimental

2.1. Materials

Composite bars (17 mm in diameter and 145 mm long) of Ti-6Al-4V reinforced by 10% vol. of TiC_p (CermeTi-C-10), produced by Dynamet Technology through cold isostatic pressing, vacuum sintering and hot isostatic pressing, were used. This material was not

submitted to plastic deformation processes before our investigations.

The chemical composition of composite matrix was determined by atomic absorption spectroscopy. To this purpose, the material matrix was dissolved by chemical etching and the analysis was performed on the obtained solution. Weight percents of 4.75 and 6.21 for V and Al respectively were measured in the matrix.

Tensile specimens and composite discs (for aging tests) were machined from the bars using diamond tools.

2.2. Methods

2.2.1. Thermal treatments

Composite specimens were isothermally treated at different temperatures in calm air or under vacuum. The treatments in stationary air were performed in a tubular furnace at 500°C, which is believed the maximum temperature at which the Ti-6Al-4V can work without undergo strong oxidation. In addition, other samples were treated in oxidizing environment at 700°C for 100 hours, with the aim of checking the thickness of the oxidized layer, grown on the surface during the thermal exposure.

These treatments, and other ones carried out in more severe conditions (higher temperatures and longer periods), were also repeated under vacuum. These last treatments were performed in order to better study the thermal stability of the ceramic/matrix interfaces. It is well known that some of the temperatures adopted in the investigation cannot be experienced by Ti-6Al-4V, otherwise they may be sustained by other titanium alloys. In order to prevent the oxidation of Ti-6Al-4V matrix, the composite samples were sealed under vacuum in silica tubes before heat treating. All the heat treatment conditions are scheduled in Table I.

2.2.2. Tensile tests

Round tensile specimens (sample length 140 mm) were machined from the as-received composite bars and submitted to tensile tests according to ASTM E8M and E21 specifications. These samples were tested at different temperatures in the range of 25–800°C. In addition, tensile specimens were aged under vacuum at 700°C for 500 h, before testing it at 25°C with the aim of investigating the effect of thermal exposure on material behaviour. Tensile tests were performed at a constant crosshead speed of 0.3 mm/min. In the case of high temperature measurements, the temperature was raised up to the prefixed value and, after a 15 minutes remaining at the set temperature, the load was applied.

The tensile strength measurements were performed by using an universal 4505 Instron apparatus equipped with an extensometer to measure the axial strain. The Instron 2620 or 2632 extensometers were used to perform tests respectively below and above 200°C. The extensometer used for high temperature tests must be removed before the sample failure in order to avoid its damage (which easily may occur, because this equipment is made of brittle quartz components). For this reason, in the case of high temperature tests, the elastic modulus was calculated by considering the slope of the initial part of the stress-strain curve and the tensile elongation was obtained by measuring the sample length after failure. The fracture surface morphology was investigated by scanning electron microscope.

TABLE I Thermal treatment conditions

Temperature (°C)	Time (h.)	Gaseous atmosphere
500	100	air; vacuum
500	200	air; vacuum
700	100	air; vacuum
700	500	vacuum
1050	100	vacuum

2.2.3. Microstructure characterization

The microstructure of composite samples was investigated by scanning electron microscope (SEM), X-ray diffraction (XRD) and electron probe microanalysis (SEM-WDS).

The microstructure of the as-processed composite was compared with those resulting from different thermal treatments. In fact, the microstructure modifications, possibly occurring during thermal exposure, fix the extreme working conditions that this composite could experience in service.

SEM analyses were carried out by using a Leica-Oxford scanning electron microscope. SEM-WDS measurements were performed by a Jeol-Superprobe JXA-8600 equipment. A TiC powder standard (Johnson Mattey, purity 99%) was used to ensure reproducibility and accuracy in carbon wt.% measurement. The LDEC crystal was used for wt. % carbon analysis, while Tapj crystal for Al (standard Al, purity 99.99%) and Pet crystal for Ti (standard TiC) and V (standard V_2O_5, Aldrich, purity 99.99%) were adopted. The K_α line was used for all elements percent determination, except for V, which was analysed by using K_β, this last being the more intense not-overlapped vanadium peak.

A PW1710 Philips diffractometer, equipped with a monochromator, was used for XRD measurements (Cu K_α radiation).

The lattice parameter of the TiC cubic cell was calculated on the basis of the diffraction angles of the more relevant TiC reflexes in the XRD patterns (Miller indexes: 111, 200 and 220). As literature data [11] permit to correlate (unfortunately with some degree of uncertainty, because of the scattering of the published experimental results) the TiC lattice parameter with the TiC chemical composition, the XRD outcomes allowed us to determine the carbon atomic percent using the graphic in Fig. 1.

3. Results and discussion

3.1. Tensile strength

The tensile characteristics of the composite measured at different temperatures in the range $25 \div 800$°C are reported in Table II.

The yield strength and the modulus value measured at 25°C are only slightly lower than those reported in literature, while the ultimate strength well agrees with literature data [12].

TABLE II Tensile properties of Ti-6Al-4V/TiC_p

Temperature (°C)	σ_u (MPa)	σ_y (MPa)	E (GPa)	Elongation (%)
25	804	779	133	0.3
200	710	605	125	0.5
400	518	—	106	1.4
500	516	—	106	1.5
600	373	—	94	1.4
800	205	—	—	6.0

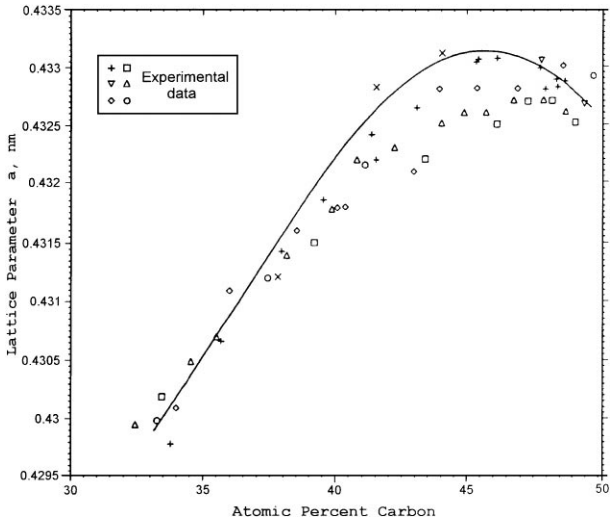

Figure 1 TiC lattice parameter variation against carbon atomic percent (adapted from [11]).

On the contrary, only an elongation of 0.3%, instead of 1%, as reported in [12], was observed. It is worthy of notice that the composite tensile strength is also lower than that declared by the producer. However, generally, this kind of composite is strengthened by plastic deformation, while we tested the material as resulted from HIP process (without any subsequent mechanical strengthening treatment).

The Young modulus value (in Table II) is very close to that reported in literature for this composite, after HIP and forging. This probably means that the elastic modulus, being primarily related to the kind of chemical bonds existing inside the two material components, and only with a minor extent to the matrix microstructure, is scarcely affected by matrix strengthening processes.

Furthermore, the measured modulus value well fits with that calculated [13] starting from the elastic constants of composite matrix and TiC (respectively 118 and 440 GPa). The results reported in Table II show that the tensile strength and the elastic modulus do not decrease in a regular way with the temperature increase.

Actually, the ultimate tensile strength decreases of about 35% in the temperature range of $25 \div 400$°C, but it remains almost constant between 400 and 500°C. Afterwards, decrements of 53% and 74%, with respect to the value measured at 25°C, occur at 600 and 800°C respectively.

The elastic modulus shows a similar trend, even though its variations are much less important. The fracture surface morphology of the composite samples appreciably changed with the tensile test temperature. The fracture surfaces of the specimens tested at 25°C (Fig. 2) show a composite brittle behaviour: only small dimples (less than 1 μm in size) inside the composite matrix can be observed and several TiC particles placed on the fracture surface are broken.

Conversely, the fracture surfaces of the specimens tested at 800°C (Fig. 3) show larger dimples in the matrix, while the ceramic particles seem to be absent on this surface, probably due to the weakening of the interfacial bonds, which caused the particles debonding during the test.

The tensile tests carried out using composite specimens previously submitted to a long period treatment under vacuum (500 h at 700°C) showed surprising results. In fact, a tensile strength of 821 MPa and a Young modulus of about 140 GPa were measured.

The measured strength value, in spite of the matrix recovery and/or recrystallization (which have to occur during a treatment at 700°C), was then slightly higher than that of the as-fabricated composite. This feature can be caused by an enhancing of the sintering degree, which probably occurred during the annealing at 700°C.

The tensile strength measured after aging at 700°C shows that the material displays a thermal stability significantly higher than that of similar titanium based composites reinforced by SiC. These other composites, which generally contains SiC long fibers, suffer of more or less important degradation phenomena when thermally aged (in not oxidizing atmosphere too) at temperature around or above 600°C.

For instance, the tensile strength of a Ti-6Al-4V/SiC_f (SCS-6 fibers) composite decreases of about 28% following a 512 h aging treatment at 595°C [14]. Also the use of protective coatings deposited on the ceramic fibers can only delay, but not avoid, detrimental matrix/SiC reactions at this temperature. The tensile strength of a Ti-6Al-4V/SiC_f material (containing Sigma fibers, coated by a $C + TiB_2$ layers) is unchanged after 360 h at 600°C, but decreases of about 39% after 1000 h at this temperature [15].

3.2. Microstructure of the as-received material

The composite sections show that the reinforcement distribution is not very homogeneous, being the particles frequently agglomerated and probably sintered; furthermore, these ceramic agglomerates present a certain degree of porosity (Figs 4 and 5). The measured density of the composite (4.15 g/cm^3) also confirms the not complete material densification, because this experimental density value is significantly lower than that calculated, from the densities of matrix and TiC, according to the rule of mixtures (4.48 g/cm^3).

However, it is to be underlined that the pores observed on the sample surface can also arise from the sample polishing, which may cause ceramic particle debonding. A rather weak interfacial bond between matrix and ceramic particles is confirmed by SEM, which puts in evidence matrix/TiC decohesion phenomena (Fig. 6).

Chemical etching of the metallographic samples enlightens a particular morphology of the titanium matrix

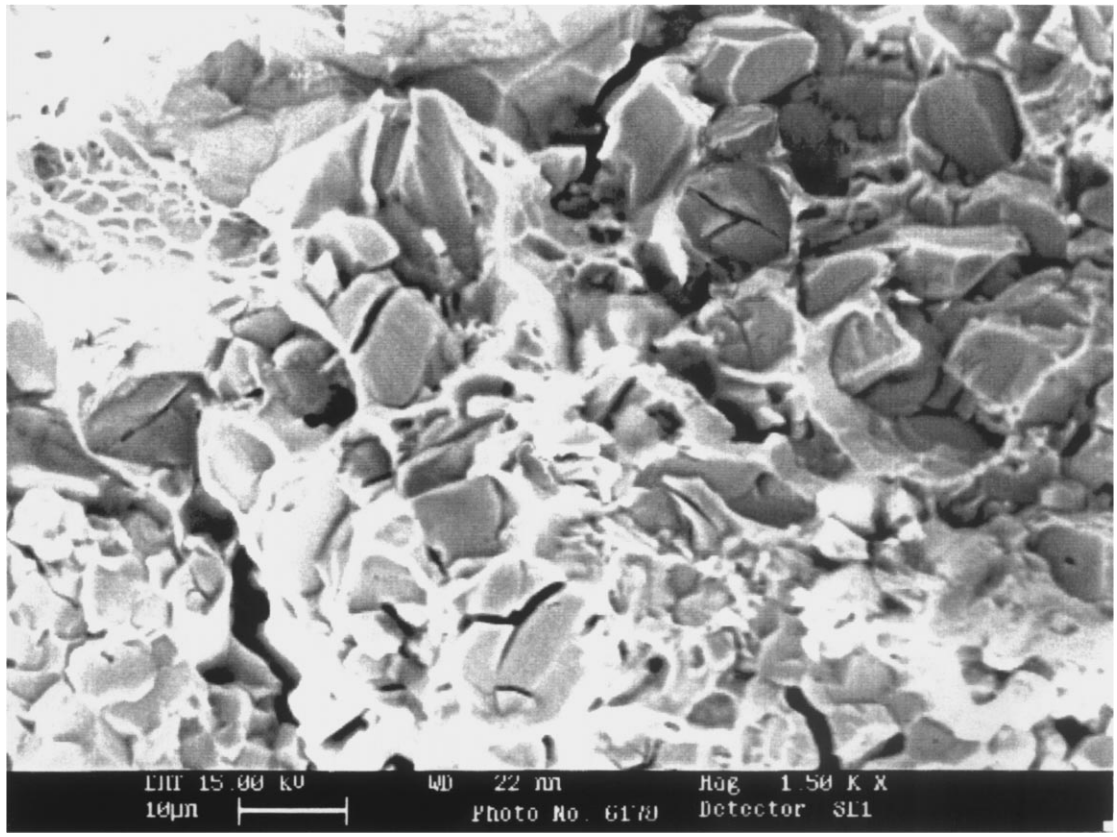

Figure 2 Fracture surface of the Ti-6Al-4V/TiC_p composite tested at 25°C.

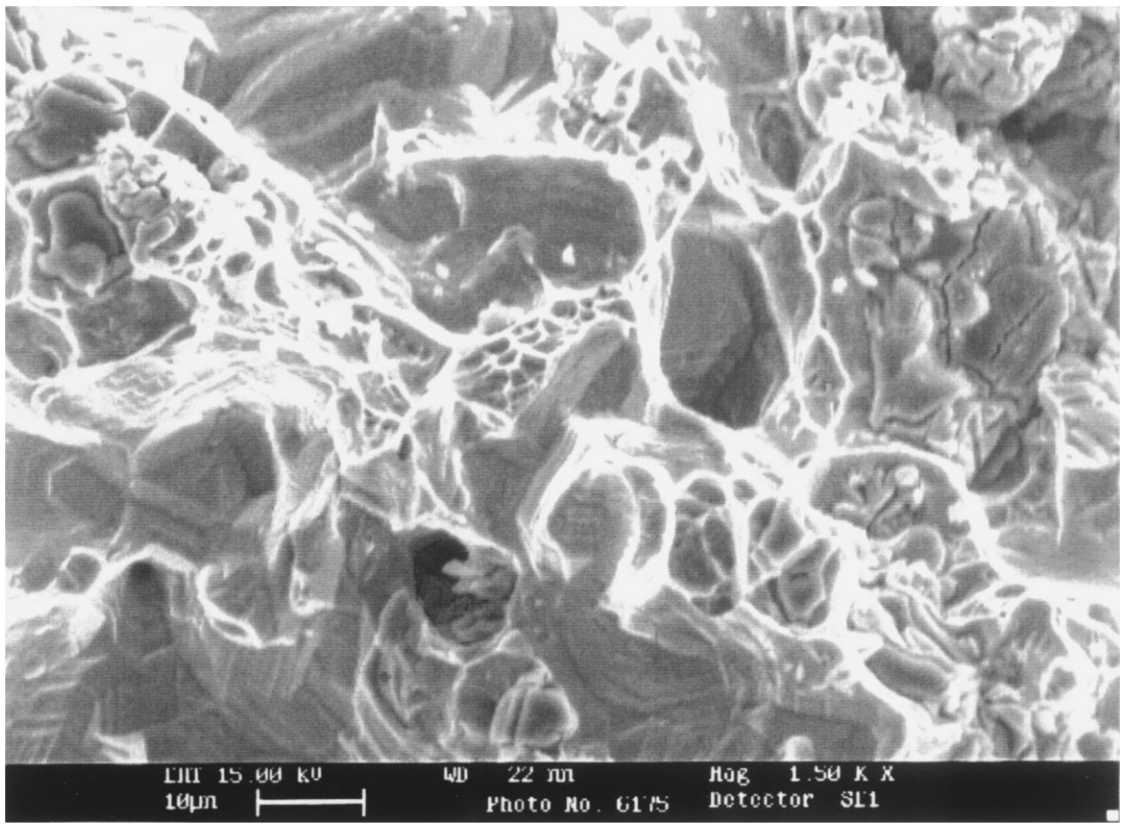

Figure 3 Fracture surface of the Ti-6Al-4V/TiC_p composite tested at 800°C.

grains. In fact a Ti-6Al-4V alloy, air cooled from more or less high temperatures, should present acicular or plate-like elongated α grains, with β phase at the grain boundaries and bigger crystals of primary α (if the cooling is carried out starting from a temperature below the β-transus). Conversely, the composite matrix contains not-elongated α grains, with β crystals at the grain boundaries (Fig. 7). The quasi-equiaxed morphology of

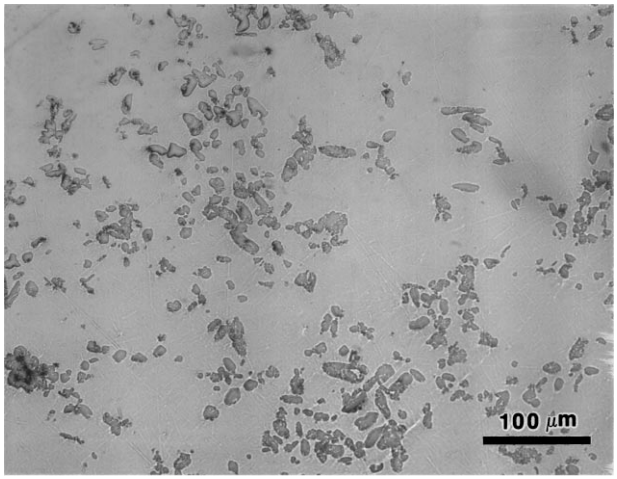

Figure 4 Ceramic particle distribution in the as-received Ti-6Al-4V/TiC_p composite (200×).

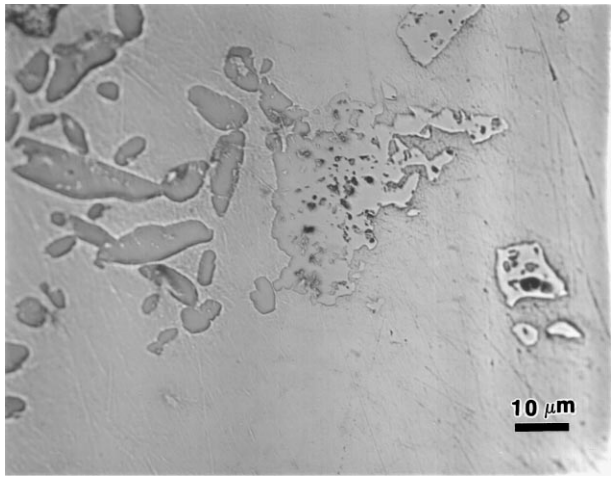

Figure 5 TiC particle porosity observed in the as-received composite (1000×).

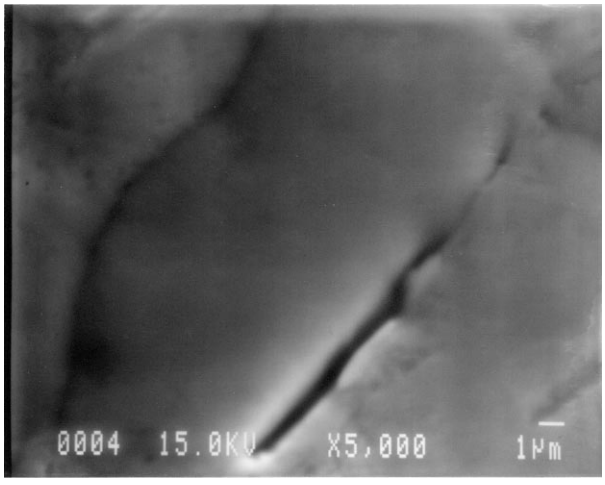

Figure 6 Ceramic particle/matrix debonding in the as-received composite.

α grains in the composite suggests that the growth of this phase from the β crystals occurs in a different way with respect to the unreinforced alloy. Very likely, the presence of ceramic particles, that is the presence of the matrix/TiC interfaces, hinders the growth of α crystals parallels to specific crystallographic planes and,

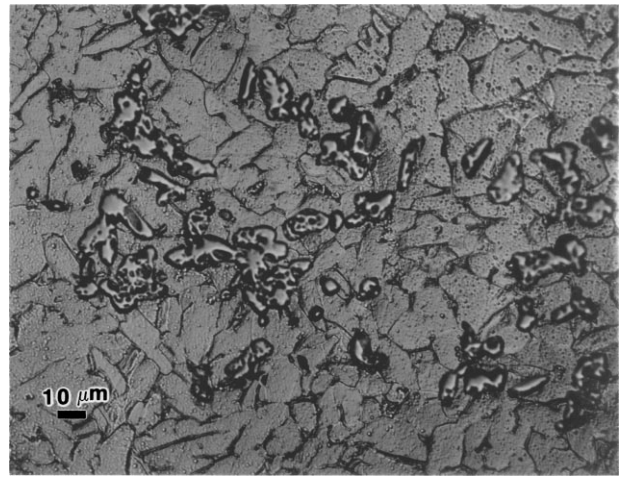

Figure 7 Morphology of the matrix grains in the as-received composite (500×; etching HNO_3 15%-HF 10%).

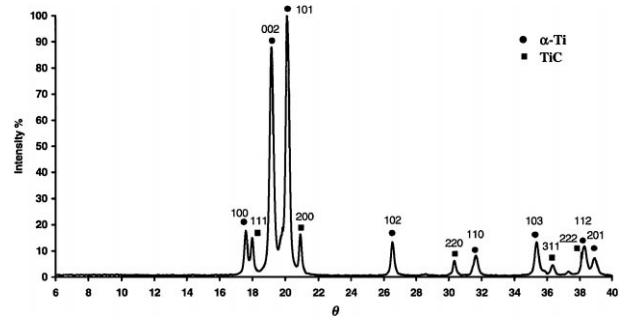

Figure 8 XRD pattern of the as-received composite.

as a consequence, the formation of elongated crystals (Widmanstatten structure).

Fig. 8 shows the characteristic diffraction pattern of the composite, where the more strong peaks pertain to the matrix or to TiC. However, other weaker peaks were occasionally observed in other spectra of the as received material; in particular a peak placed between $\theta = 14 \div 15$ was detected, which was tentatively attributed to a carbide of formula Ti_2C (as discussed in the following).

3.3. Microstructure of treated samples

3.3.1. Metallography

The specimens treated under vacuum at 500 and 700°C show a microstructure similar to that of the as-received material. In fact, quasi-equiaxed crystals of α-titanium with β-phase segregated at the grain boundaries are present in the metal matrix, while neither reaction interlayers or precipitates can be detected at the matrix/ceramic interface.

Grain growth of α-titanium during some thermal treatments occurs, but this phenomenon does not change the crystal shape, which remains very different from that expected for a $\alpha + \beta$ titanium alloy air cooled from the $\alpha + \beta$ field. Moreover, the presence of ceramic particles probably slows down the grain growth process, in fact this last phenomenon is well appreciable only after a 500 h treatment at 700°C (Fig. 9).

The bulk microstructure of samples aged in air (at 500 or 700°C) is similar to that of samples treated under

vacuum. However, the former specimens show the formation of a surface oxidation layer, which is only few μm thick in the case of samples treated at 500°C but more than 400 μm thick for the samples kept 100 h at 700°C. The growth of this surface layer, which is prone to undergo exfoliation phenomena, confirms that the Ti-6Al-4V matrix prevents the use of this composite above 500°C, even though the interfaces between titanium matrix and TiC particles seems to be very stable also at higher temperatures (at least up to 700°C).

On the other hand, microstructure variations were observed in composite samples aged for 100 h at 1050°C. In this last case the interface matrix/TiC is unchanged (Fig. 10), but the metal matrix suffers of heavy modifications.

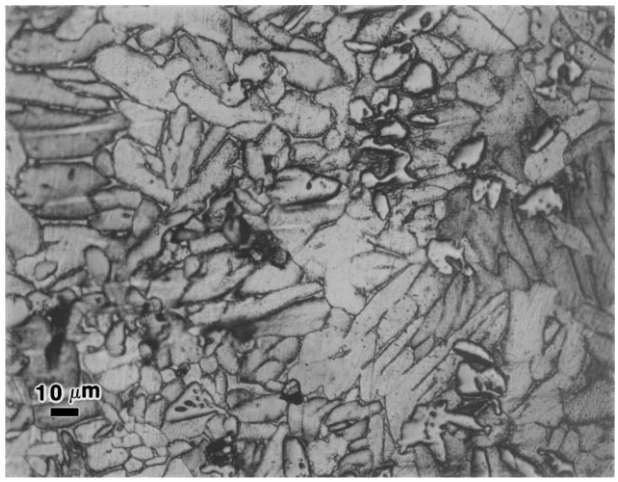

Figure 9 Matrix grain growth after 100 h at 700°C (500×; etching HNO_3 15%-HF 10%).

In this extreme aging condition titanium evaporates from the composite and deposites on the walls of the silica tube containing the samples; this evaporation/condensation phenomenon results in the formation of porosity inside the composite matrix.

The XRD analysis of the powder material deposited on the walls of the tube shows that it is chiefly constituted of Ti_5Si_3, TiO_2 and Ti. The loss of titanium through an evaporation-condensation mechanism very probably is aided by the following reaction between titanium and silica:

$$8Ti + 3SiO_2 \rightarrow Ti_5Si_3 + 3TiO_2$$

Inside the matrix new phases precipitates, preferentially around the pores, also because of the strong changes occurring for the matrix chemical composition (Fig. 11).

3.3.2. X-ray diffraction

The XRD patterns of the samples treated under vacuum at temperatures of 500 and 700°C (for periods up to 200 and 500 h respectively) show the progressive growth of a new diffraction peak which can be tentatively attributed to the compound Ti_2C. This peak has appreciable intensity after aging of 200 h at 500°C and, much more, after a treatment of 500 h at 700°C (Fig. 12).

The XRD spectra of the oxidized layer formed on specimens treated in air show that this surface layer is chiefly constituted of TiO_2, even though weaker peaks pertaining to TiN can also be detected.

After the removal of the oxidized layer by mechanical polishing, the XRD analysis was repeated, obtaining

Figure 10 TiC/matrix interface after a thermal treatment at 1050°C.

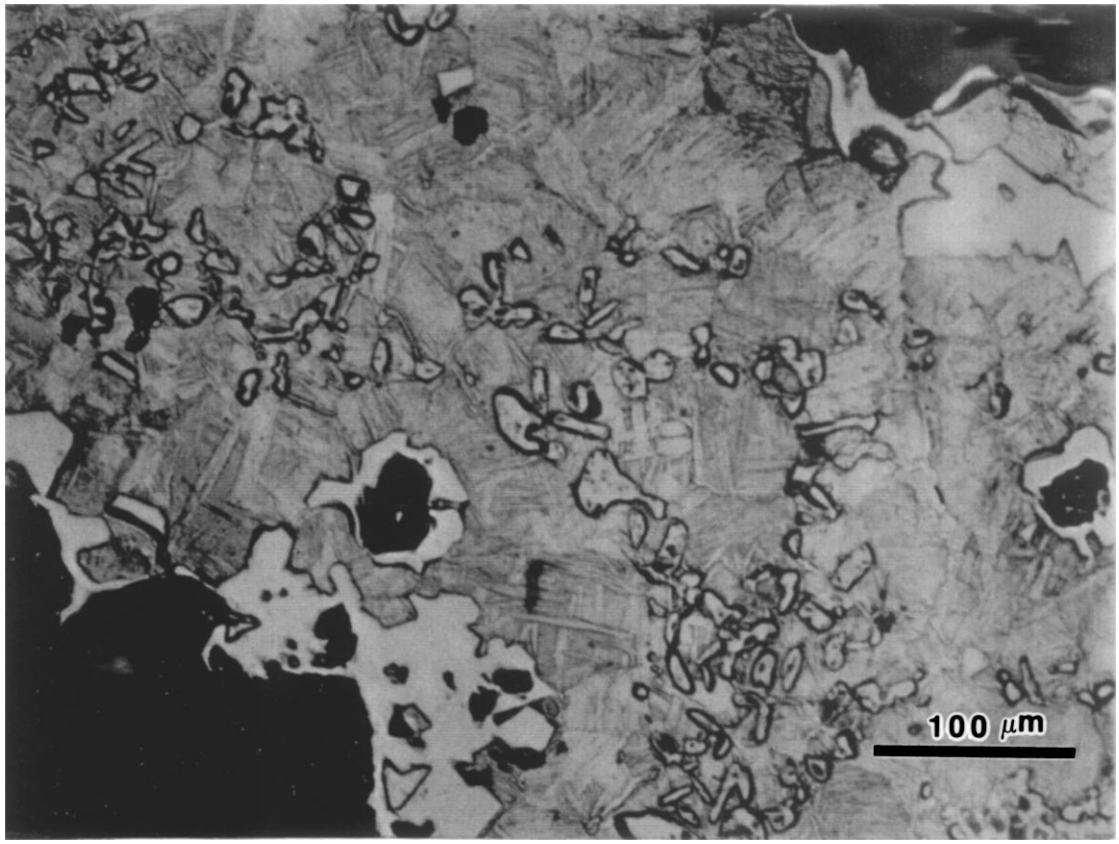

Figure 11 New phase formation around matrix pores after the treatment at 1050°C.

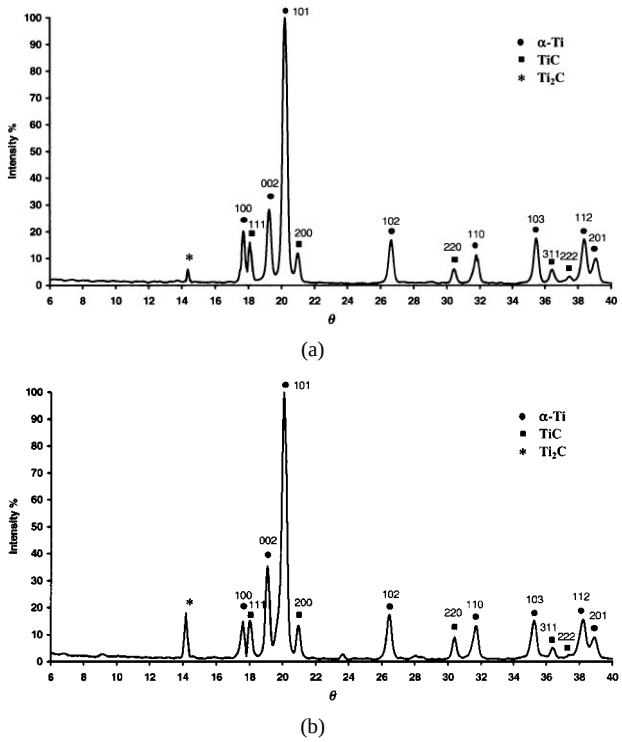

Figure 12 XRD pattern of composite sample after vacuum thermal treatments: a = 200 h at 500°C; b = 500 h at 700°C.

patterns coincident with those recorded for samples aged under vacuum in the same conditions of time and temperature. In fact, these spectra contain only the diffraction peaks of Ti, TiC and that previously attributed to Ti_2C.

The existence of the Ti_2C is not well assessed because most of Authors do not consider TiC and Ti_2C as distinguished phases, even though this last carbide is sometimes reported in the TiC phase diagram [11] (Fig. 13). The lattice parameter of TiC progressively changes with its carbon content: the cubic cell of this not-stoichiometric compound becomes smaller with the carbon content decrease from 49 to about 32 atomic percent. When the carbon content decreases toward the lower limit a new crystalline ordered structure is believed to form (namely Ti_2C). The possible crystal structure of Ti_2C has been reported in literature [11, 16]: space group Fd3m, with carbon atoms in the 16 (c) and titanium atoms in the 32 (e) positions, lattice parameter of 0.86 nm, that is twice than that of TiC. Diffraction peaks corresponding to Ti_2C were observed by TEM [17, 18] or by neutron diffraction (superlattice

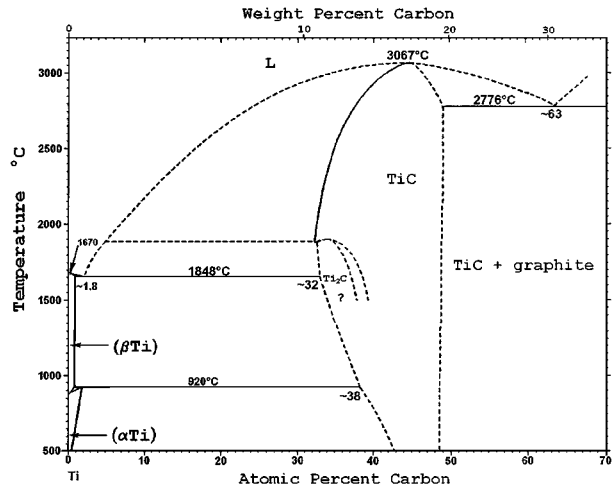

Figure 13 Ti-C phase diagram (adapted from [11]).

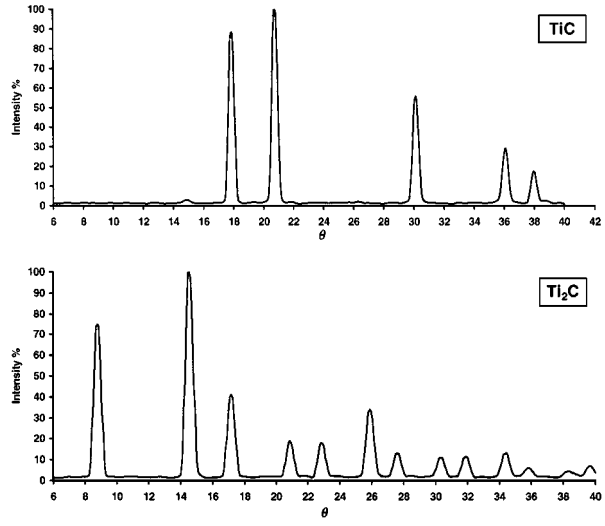

Figure 14 Calculated XRD patterns of: TiC and Ti_2C.

lines) [16] in samples of a Ti-6Al-4V/TiC composite aged at high temperature. Unfortunately, the X-ray diffraction pattern of the pure Ti_2C was never experimentally recorded and, consequently, reported in literature.

We calculated the XRD pattern of Ti_2C according to the crystalline structure proposed by some Authors [11, 16]. The computed XRD spectrum (Cu K_α wavelength) is compared (Fig. 14) with that calculated, with the same computer program, for TiC (space group Fm3m).

Actually, the strongest Ti_2C reflex, which is placed just above $\theta = 14$, well corresponds to the peak that progressively grow in the experimental patterns of our aged samples. However, the calculated Ti_2C spectrum also shows other peaks lying in the range $\theta = 8$–28. Most of these calculated peaks should be overlapped with those of titanium or TiC, but it is not the case of the peak placed at $\theta = 8 \div 9$, which was never observed in the patterns of the composite under investigation. For this reason, the formation of the Ti_2C carbide in the aged Ti-6Al-4V/TiC composite still remains doubtful.

XRD analysis allowed us to evaluate the change of the TiC lattice parameter occurring during composite aging. In addition, the atomic percent of carbon in TiC was calculated from the lattice parameter value by using the curve in Fig. 1. Both the lattice parameter and the corresponding carbon percent are reported in Table III for some untreated and aged composite samples.

The results in Table III show that carbon content in the TiC particles only slightly changes with both treatment temperature and time. However, the carbon percent calculated according to XRD method has to be regarded as an average value; while a progressive carbon diffusion, possibly occurring from the TiC particle core toward the particle/matrix interface, may be observed by microprobe analysis only.

The composite vacuum treatment carried out at 1050°C results in a complex sample diffraction pattern (Fig. 15), chiefly because of the formation of new carbides: Ti_3AlC, $Ti_4Al_2C_2$ and (possibly) Ti_2C. Furthermore, it was not possible to assign all the diffraction peaks to specific compounds, even though some weak

TABLE III Lattice parameter and carbon content of TiC in composite specimens treated in different conditions

Sample treatment				
Temperature (°C)	Time (h.)	Atmosphere	a_0 (Amstrong)	Carbon content (% at.)
	None		4.318	39
500	100	air	4.314	38
500	200	air	4.311	36
500	200	vacuum	4.307	35.5
700	100	vacuum	4.306	35
1050	100	Vacuum	4.312	37

reflexes in this spectrum may be ascribed to titanium oxides (probably formed by reaction between the sample matrix and the silica tube or the gaseous oxygen diffusing through the tube walls during the high temperature treatment).

In this XRD spectrum the position of the Ti_3AlC characteristic diffraction peaks are often very close to those of TiC. In order to distinguish partially overlapped peaks, pertaining to different carbides, the θ scale must be enlarged as shown in Fig. 16. This figure shows that some diffraction peaks are structured and puts in evidence the possible formation of the V_8C_7 carbide too.

In conclusion, XRD analyses show that chemical reactions between the two components of the material occur only starting from temperatures above 700°C.

3.3.3. Electron probe microanalysis

A possible carbon concentration variation across the TiC particle was investigated by repeating the WDS analysis in different points of the ceramic particles, that is moving from their center towards the TiC/matrix interface. Actually, it was never observed a concentration gradient: the carbon content was almost constant inside the carbide particles and suddenly fell when the electron beam was positioned in the matrix close to the reinforcement. However, the carbon percent may slightly change when different particles or different parts of a single particle are analyzed, even though these small variations do not show a clear trend. The average percents of carbon measured for the TiC particles contained in each composite sample are compared in Table IV. These results confirm that the carbon percentage in the ceramic particle is scarcely affected by the composite thermal treatments. Furthermore, the carbon content in the TiC particles is always well below the upper limit of 49% at. Hence, it can be inferred that carbon diffusion occurs from the particles towards the matrix since the composite processing. The results of WDS analysis performed on the metal matrix strengthen this hypothesis (Table V).

The metal matrix composition changes point by point because it contains two phases (α and β). In order to measure the overall matrix composition the electron beam was widened (higer beam current), the analysis was repeated several times and the results were averaged. The average atomic percents of carbon is always greater than 1% at., that is well above the normal value for a Ti-6Al-4V alloy. Furthermore, these measured

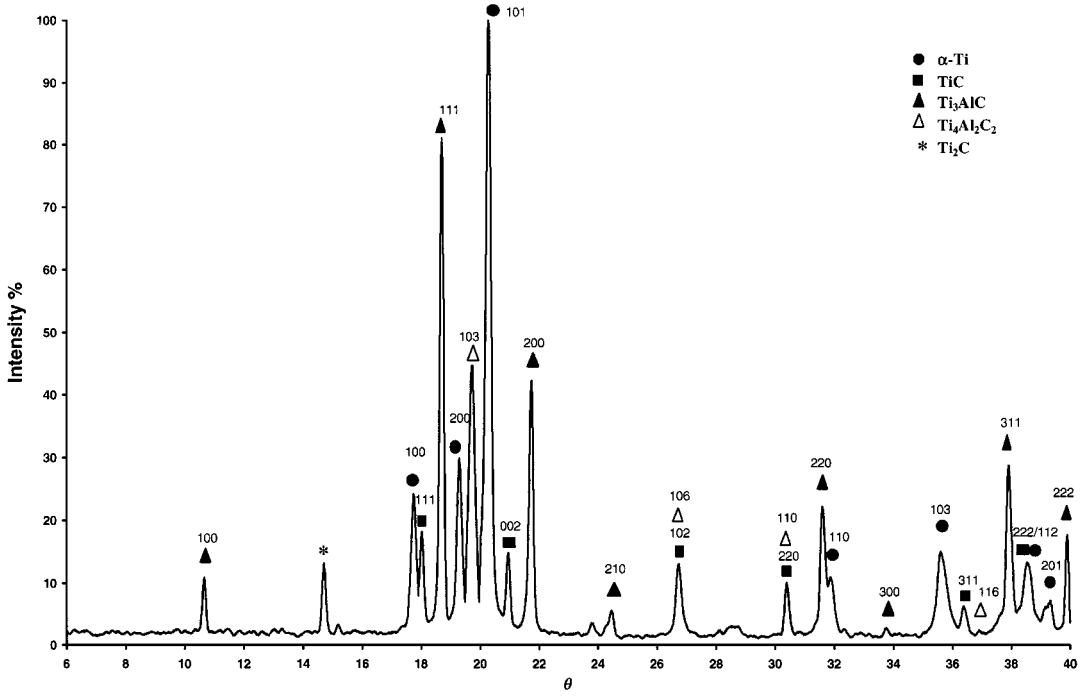

Figure 15 XRD pattern of the composite after 100 h at 1050°C under vacuum.

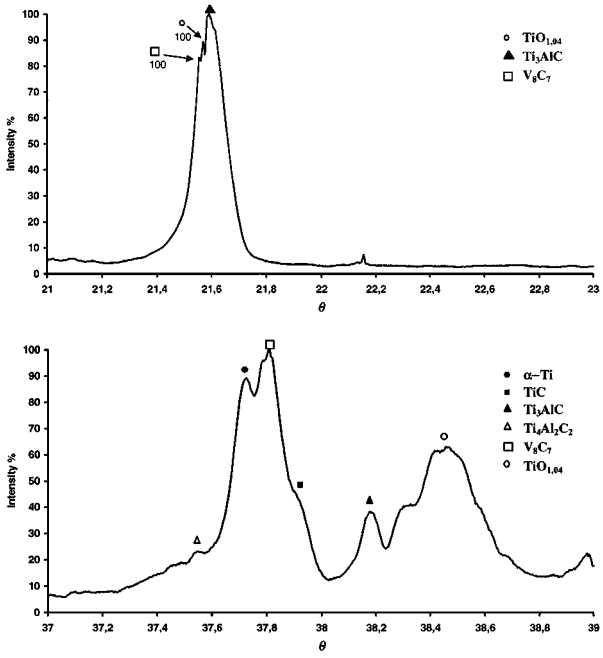

Figure 16 Partially overlapped diffraction peaks of different phases present in the composite samples aged at 1050°C.

values are higher than the equilibrium one reported in the Ti-C phase diagram at room temperature and they frequently are close to the maximum solubility of carbon in titanium (about 1,6% at. achieved just at 920°C [11]). Very likely, following the rapid cooling of the composite from the processing temperature and/or from the thermal treatment temperatures, metastable supersaturated solid solutions of carbon in the titanium were obtained.

The WDS analysis results for the different phases present in the composite annealed at 1050°C are shown in Table VI. Poor accuracy has to be attributed to the measured vanadium content because the K_α line of this element is overlapped to the K_β line of titanium and, consequently, only weak vanadium lines in the X-ray spectrum can be used to measure its percentage with WDS technique. This feature also frustrate the possibility to identify small precipitates of vanadium carbide.

On the contrary, microprobe analysis confirms that, in particular around the pores resulting from titanium evaporation, Ti-Al carbides form.

In addition, precipitates containing an appreciable amount of silicon were occasionally observed inside the metal matrix of the sample annealed at 1050°C (Table VI).

TABLE IV Carbon content of TiC particles

	Atomic %	Weight %
As received	34.15	11.39
200 hours at 500°C	34.05	11.62
100 hours at 700°C	34.45	11.40
100 hours at 1050°C	34.95	11.94

TABLE V Carbon content of composite matrix

	Atomic %	Weight %
As received	1.56	0.45
200 hours at 500°C	1.51	0.40
100 hours at 700°C	1.13	0.32
100 hours at 1050°C	1.33	0.37

4. Conclusions

Some major conclusions about the high temperature behaviour of Ti-6Al-4V/TiC_p (CermeTi-C-10) can be drawn, as listed in the following.

- CermeTi-C-10 composite shows at 25°C tensile strength similar to that of the unreinforced alloy,

TABLE VI Composition of observed phases in material heat treated at 1050°C, weight % and atomic %

	Ti		Al		V		C		Mg		Si	
	% w	% at	% w	% at	% w	% at	% w	% at	% w	% at	% w	% at
Matrix	88.93	83.57	7.23	12.02	3.47	3.08	0.37	1.33	—	—	—	—
TiC particle	87.59	64.54	0.28	0.38	0.19	0.13	11.94	34.95	—	—	—	—
Reaction phase (near pores)	82.21	67.73	13.28	18.99	0.48	0.36	4.03	12.92	—	—	—	—
Unidentified phase	43.46	35.39	4.92	7.13	1.54	1.17	0.37	1.37	14.67	17.91	35.04	37.03

but better stress-strain properties (modulus and strength) at high temperatures.

- This composite is suitable for working in air up to 500°C only, due to the oxidation of metal matrix.
- The adoption as composite matrix of a titanium alloy more stable in an oxidizing environment than Ti-6Al-4V probably enables composite applications at higher temperature, because of the noticeable thermal stability of the TiC/Ti interface.
- Long period treatments up to 700°C (500 h) don't cause the diffusion of carbon from TiC toward the matrix (which contains a carbon percent near the maximum solubility) or the formation of a ceramic-matrix reaction layer.
- Aging at 700°C does not change the composite tensile strength.
- Chemical reactions between TiC and titanium matrix occur at 1050°C: at this temperature new Al-Ti carbides form.
- Then Ti-6Al-4V/TiC composite shows better thermal stability than the more popular titanium/SiC composites, which experience detrimental reactions at the interface between the two material components starting from 600°C.

References

1. F. H. FROES and D. EYLON, *Int. Met. Rev.* **35** (1990) 162.
2. Z. FAN, H. J. NIU, A. P. MIODOWNIK, T. SAITO and B. CANTOR, "Key Engineering Materials Vols. 127–131" (Trans. Tech. Publication, Switzerland, 1997) p. 423.
3. T. SAITO, T. FURUTA and T. YAMAGUCHI, in "Recent Advances in Titanium Metal Matrix Composites," edited by F. H. Froes and J. Storer (The Minerals, Metals & Materials Society, 1995) p. 33.
4. T. SAITO, *Advanced Performance Materials* **2** (1995) 121.
5. T. SAITO, T. FURUTA and I. TAHAMIYA, in Proceedings of the Eight World Conf. on Titanium, Birmingham, U.K., 22–26 October 1995, p. 2763.
6. S. ABKOWITZ, P. F. WEINBRAUCH and S. M. ABKOWITZ, in "Powder Metallurgy and Particulate Materials, Vol. 6: Speciality Materials and Composites Advances" (Metal Powder Industries Federation, Princeton, N.J., USA, 1993) p. 121
7. S. ABKOWITZ, P. F. WEINBRAUCH and S. M. ABKOWITZ, *Industrial Heating* **60** (1993) 32.
8. S. ABKOWITZ, P. F. WEINBRAUCH, S. M. ABKOWITZ and H. I. HEUSSI, *JOM* **47** (1995) 40.
9. S. ABKOWITZ and P. F. WEINBRAUCH, *Adv. Mat. & Proc.* **7** (1989) 31.
10. S. ABKOWITZ, P. F. WEINBRAUCH, H. L. HEUSSI and S. ABKOWITZ, in Proc. of the Eighth World Conference on Titanium, Birmingham, U.K., 22–26 October 1995, p. 2722.
11. J. L. MURRAY (ed.), "Phase Diagram of Titanium Binary Alloys" (ASM International, Metals Park, Ohio, 1987) p. 47.
12. "ASM Metals Handbook Vol. 2," 10th ed. (The Materials Information Society, Metal Park, Ohio, 1990) p. 650.
13. L. LUTEROTTI, G. ELVATI and S. GIALANELLA, in Atti 3° Cong. Nazionale AIMAT, Napoli, 25–27 Settembre 1996, edited by C. COLELLA (A. De Freda, Napoli, 1996) Vol. II, p. 725.
14. P. R. SMITH, F. H. FROES and J. T. CAMMET, in Proceedings of Int. Conf. on Mechanical Behaviour of MMCs, Dallas, 16–18 February 1982, edited by W. D. Brewer and J. Unnam (The Metallurgical Society AIME, 1982) p. 143.
15. C. BADINI, P. APPENDINO, F. MARINO and E. VERNÈ, in "Advanced Structural Fiber Composites," edited by P. Vincenzini (Techna, Faenza, Italy, 1995) p. 85.
16. H. GORETZKI, *Phys. Stat. Solidi—Short Notes* **20** (1967) K 141.
17. M. H. LORETTO and D. G. KONITZER, *Metall. Trans.* A **21** (1990) 1579.
18. P. WANJARA, S. YUE, R. A. L. DREW, J. ROOT and R. RONABERGER, "Key Engineering Materials, Vols. 127–131" (Trans. Tech. Publication, Switzerland, 1997) p. 415.

Received 13 May 1999
and accepted 1 February 2000